Article

Journal of the Brazilian Chemical Society

https://dx.doi.org/q10.21577/0103-5053.20230165

J. Braz. Chem. Soc. **2024**, *35*, 4, e-20230165, 1-6

$FeCl_3$-Catalyzed Cross-Coupling for Improving the Synthesis of Upadacitinib

*Ziling Li,[a] Chundiao Shi,[a] Shengchang Xiang,[a] Chulong Liu *[,a] and Ximing Zheng *[,b]*

[a]*Fujian Provincial Key Laboratory of Polymer Materials, College of Chemistry and Materials Science, Fujian Normal University, 8 Xuefu South Road, Fuzhou 350117, China*

[b]*Fujian Provincial Key Laboratory of Eco-Industrial Green Technology, Key Laboratory of Green Chemical Technology of Fujian Province University, Wuyi University, Wuyishan 354300, China*

As an oral Janus kinase 1 inhibitor, upadacitinib shows good activity in the treatment of rheumatoid arthritis, especially for other drug-resistant and refractory rheumatoid arthritis patients. A key step in the synthesis of upadacitinib is the introduction of ethyl on the pyrroline ring. Here, a $FeCl_3$/*p*-aminophenol catalyst system was used to increase the ethyl introduction for synthesis of pyrroline building blocks of upadaticinib. This catalytic system allows milder reaction conditions and increases the yield of this step by 25% compared to the existing reports, and the scale-up experiment is still effective. In addition, a possible Fe^{II}/Fe^{IV} catalytic mechanism for this reaction was also proposed.

Keywords: iron catalysis, *p*-aminophenol, cross-coupling, upadaticinib, synthesis

Introduction

Rheumatoid arthritis (RA) is a systemic autoimmune disease of unknown etiology characterized by progressive joint destruction through chronic synovitis, resulting in joint deformity and partial loss of function.[1,2] Any joint in the body can be affected by rheumatoid arthritis. However, it primarily affects the proximal interphalangeal, metacarpophalangeal, and metatarsophalangeal joints of the wrist and knee.[3] Studies[1-3] have shown that in autoimmune inflammatory diseases such as RA, Janus kinase (JAK) enzymes play an important role in the regulation of the immune system due to their involvement in cytokine signaling. There are four protein tyrosine kinases in the JAK family associated with RA, mainly JAK1, JAK2, JAK3, and protein tyrosine kinase 2 (TYK2).[4-8] The development of JAK inhibitors is mainly to inhibit the activity of one or several Janus kinases. Upadacitinib (Figure 1) is an oral JAK1 inhibitor for the treatment of RA and other immune-mediated inflammatory diseases.[9] Clinical data have also demonstrated that upadacitinib has good efficacy for other drug-resistant and refractory RA patients.[10]

The reported synthetic route of upadacitinib is divided into pyrrolo[3,2-*b*]pyridine (**2**) part, pyrroline derivative (**3**) part, and trifluoroethyl urea structure (Scheme 1) according to the structure. The introduction of the ethyl group can be divided into introduction from the substrate when constructing the pyrroline ring (Scheme 2a);[11-13] or construct the pyrrole ring first, and then introduce the ethyl group by cross-coupling reaction (Scheme 2b).[14-18] In comparison, Scheme 2b is easier to implement, because compound **5** can be easily constructed from common chemical raw materials glycine and ethyl acrylate through Michael addition and condensation reactions (Scheme S1, Supplementary Information (SI) section), so the study of the cross-coupling step is very important for the synthetic improvement of **1**. In many synthesis patents of **1**, the cross-coupling mainly uses Pd^{II} as the catalyst,[14,15] and Ni^{II} as the catalyst in some cases,[16] but they all need to employ phosphine ligands to make the reaction go smoothly. When using ethyl boronic acid or its derivatives as the ethyl source, more than 4 equivalents of boronic acid is needed. Fe^{III} is also used as catalyst in

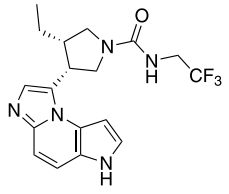

Upadacitinib (**1**)

Figure 1. Structure of upadacitinib.

*e-mail: liucl@fjnu.edu.cn; zxm70@wuyiu.edu.cn
Editor handled this article: Brenno A. D. Neto

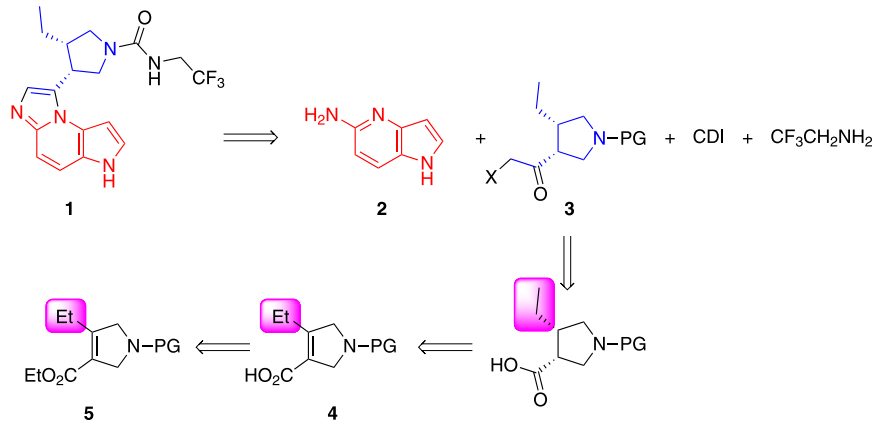

Scheme 1. Retrosynthetic analysis of upadacitinib (PG: protecting group; CDI: carbonyl diimidazole).

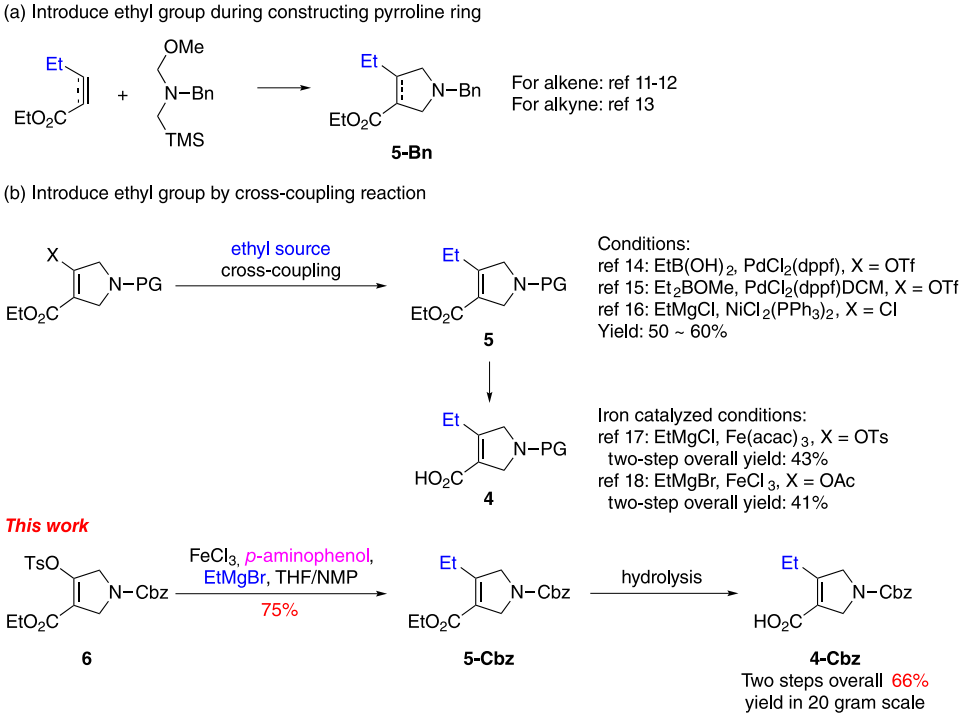

Scheme 2. Previous works[11-18] and this work scheme for 3-ethyl introduction.

other methods,[17,18] but their overall yields of producing **5** and hydrolysis to **4** do not exceed 45%, which has great potential for optimization.

It can be seen that in the synthesis of upadacitinib, the improvement of this step can improve the yield and reduce the production cost. Here, we report a $FeCl_3$/*p*-aminophenol catalyzed combination for the introduction of an ethyl group for pyrrolidine 3-position cross-coupling in the synthesis of upadacitinib. This is the first time that *p*-aminophenol has been introduced as a ligand into the iron-catalyzed system, and our method has a higher yield than previous methods.[14-18] We carried out detailed conditional experiments on this reaction and proposed the mechanism of the reaction.

Results and Discussion

Considering the reactivity, availability and cost of the reactants, 1-benzyl 3-ethyl 4-(tosyloxy)-2,5-dihydropyrrole-1,3-dicarboxylate (**6**) and EtMgBr were selected as model substrates to test the reaction conditions. The combination of $FeCl_3$/*p*-aminophenol was selected as a catalytic system for the solvents and temperature because *p*-aminophenol may facilitate the reduction of Fe^{III} to reactive Fe^{II}. As shown in Table 1, the results in entries 1-7 indicated that a good yield can be obtained when the reaction is carried out at –30 °C, in tetrahydrofuran (THF) in the absence of *N*-methyl-2-pyrrolidone (NMP) as cosolvent. NMP can also be used as a solvent for the reaction, but,

unexpectedly, only traces of product were formed when the solvent was *N*,*N*-dimethylformamide (DMF) which is also an amide. Entry 8 indicates that the yield can be improved when using NMP as a cosolvent, because NMP can stabilize the organoiron intermediates.[19] In reaction time tests (Table 1, entries 8-10), we found that 1 h was sufficient for the reaction to proceed completely. But then, we unexpectedly found that after 1 h reaction at –30 °C, if the reaction mixture was stirred at room temperature for another 1 h, the yield increased (Table 1, entry 11). After further tests on the reaction time and the amount of NMP used (Table 1, entries 11-17), we determined that the reaction time was 1 h at –30 °C, followed by 2 h at room temperature, and the amount of NMP was 1% (v/v). The experiment of the amount of reactant (Table 1, entries 18-20) showed that the most appropriate molar ratio of **6** and Grignard reagent is 1:1.8.

After determining the optimal reaction temperature, solvent and reaction ratio, the catalytic system was also studied. As shown in Table 2, the results in entries 1-4 indicate that among the transition metal elements of the same period, copper and cobalt have catalytic activity, but not as good as iron, while nickel cannot catalyze the reaction. As for ligands, the reaction requires ligands to improve the catalytic activity of iron (Table 2, entry 5), but strong coordination bidentate ligands such as 2,2'-bipy, *o*-aminophenol, 1,10-phenanthroline are not effective (Table 2, entries 8, 9 and 12, respectively). When acetylacetone, *m*-aminophenol or *p*-aminophenol is used as the ligand, they can better promote the reaction (Table 2, entries 7, 10 and 11). Among them, the ligand with the best catalytic effect is *p*-aminophenol, and the optimal catalyst usage is 2 mol% $FeCl_3$ and 4 mol% *p*-aminophenol. Under this standard condition, **4-Cbz** was prepared in 66% yield (including cross-coupling and hydrolysis) on a 20 g scale (Scheme 3), 50% higher than that reported in the literature (43 and 41%) using $Fe(acac)_3$, acac: acetylacetonate, as catalyst.[17,18]

The mechanism of iron-catalyzed cross-coupling reactions has been widely discussed. The current mainstream

Table 1. Effects of EtMgBr equivalent, solvents, temperature and reaction time in the synthesis of compound **5-Cbz**[a]

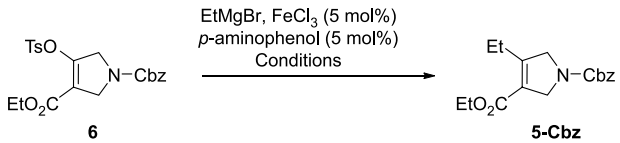

6 **5-Cbz**

entry	EtMgBr / equiv.	Solvent / mL	Temperature / °C	time / h	Yield[b] / %
1	1.8	THF (10)	–10	1	trace
2	1.8	THF (10)	–20	1	25
3	1.8	THF (10)	–30	1	30
4	1.8	THF (10)	–40	1	22
5	1.8	NMP (10)	–30	1	27
6	1.8	DMF (10)	–30	1	trace
7	1.8	THF (10) + DMF (0.1)	–30	1	30
8	1.8	THF (10) + NMP (0.1)	–30	1	37
9	1.8	THF (10) + NMP (0.1)	–30	0.5	21
10	1.8	THF (10) + NMP (0.1)	–30	2	38
11	1.8	THF (10) + NMP (0.1)	–30	1 h then r.t. 1 h	41
12	1.8	THF (10) + NMP (0.1)	–30	1 h then r.t. 2 h	70
13	1.8	THF (10) + NMP (0.1)	–30	1 h then r.t. 4 h	71
14	1.8	THF (10) + NMP (0.05)	–30	1 h then r.t. 2 h	50
15	1.8	THF (10) + NMP (0.2)	–30	1 h then r.t. 2 h	61
16	1.8	THF (10) + NMP (0.5)	–30	1 h then r.t. 2 h	44
17	1.8	THF (20) + NMP (0.2)	–30	1 h then r.t. 2 h	35
18	2.0	THF (10) + NMP (0.1)	–30	1 h then r.t. 2 h	70
19	1.6	THF (10) + NMP (0.1)	–30	1 h then r.t. 2 h	65
20	1.4	THF (10) + NMP (0.1)	–30	1 h then r.t. 2 h	31

[a]To a solution of $FeCl_3$ (5 mol%), *p*-aminophenol (5 mol%) and **6** (1 mmol) in given solvent was added EtMgBr (2.0 M in THF, given equiv.) and the mixture was stirred for given temperature and time; [b]isolated yields. r.t.: room temperature; THF: tetrahydrofuran; NMP: *N*-methyl-2-pyrrolidone; DMF: *N*,*N*-dimethylformamide.

Table 2. Effects of catalysts and ligands in the synthesis of compound **5-Cbz**[a]

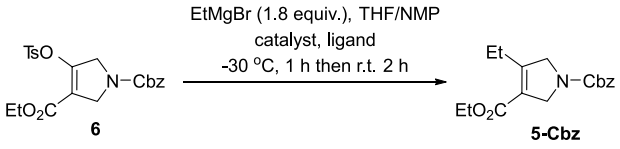

entry	Catalyst / mol%	Ligand / mol%	Yield[b] / %
1	$Fe(acac)_3$ (5)	–	49
2	$Co(acac)_2$ (5)	–	27
3	$Ni(acac)_2$ (5)	–	trace
4	$Cu(acac)_2$ (5)	–	29
5	$FeCl_3$ (5)	–	10
6	$Fe(acac)_3$ (5)	*p*-aminophenol (10)	35
7	$FeCl_3$ (5)	acetylacetone (10)	41
8	$FeCl_3$ (5)	2,2'-bipy (10)	5
9	$FeCl_3$ (5)	*o*-aminophenol (10)	14
10	$FeCl_3$ (5)	*m*-aminophenol (10)	35
11	$FeCl_3$ (5)	*p*-aminophenol (10)	59
12	$FeCl_3$ (5)	1,10-phenanthroline (10)	26
13	$FeCl_3$ (5)	aniline (10)	24
14	$FeCl_3$ (5)	phenol (10)	28
15	$FeCl_3$ (5)	pyridine (10)	15
16	$FeCl_3$ (5)	*m*-aminophenol (5)	59
17	$FeCl_3$ (5)	*p*-aminophenol (5)	70
18	$FeCl_3$ (2)	*p*-aminophenol (2)	50
19	$FeCl_3$ (2)	*p*-aminophenol (4)	75
20	$FeCl_3$ (10)	*p*-aminophenol (10)	40
21	$FeCl_2$ (2)	*p*-aminophenol (4)	55
22	$FeCl_2$ (2)	–	33

[a]To a solution of given catalyst and ligand and **6** (1 equiv.) in THF/NMP (100:1 v/v) was added EtMgBr (2.0 M in THF, 1.8 equiv.) and the mixture was stirred at –30 °C for 1 h and slowly raise to room temperature for 2 h; [b]isolated yields. acac: acetylacetonate; bipy: bipyridine.

view is that Fe^{III} generates an "inorganic Grignard reagent" $Fe(MgX)_2$ (X = halogen anion) under the action of Grignard reagent.[20] In $Fe(MgX)_2$, magnesium and iron form small clusters with metallic bonds.[21] Ar–X undergoes oxidative addition with $Fe(MgX)_2$ (formally Fe^{-II}) and substitutes with RMgX to form $Fe(MgX)_2ArR$ (formally Fe^0), which then undergoes reductive elimination to from Ar–R and $Fe(MgX)_2$ for a new round of catalytic cycle.[21] But recently, Nakamura and co-workers[22] proposed Fe^{II}/Fe^{IV} mechanism when studying FeF_3 and 1,3-bis(2,6-diisopropylphenyl) imidazolin-2-ylidene (SIPr) catalyzed cross-coupling of aryl halides with Grignard reagents, which is more suitable for explaining the mechanism of our reaction. In Nakamura's study, Fe^{III} was first reduced to Fe^{II} by SIPr, and then coordinated with SIPr as the catalytic active center. *para*-Aminophenol also has the ability to reduce Fe^{III} and coordinate with Fe^{II}, and affects the yield of the reaction. In addition, $FeCl_2$ also has the ability to catalyze the reaction and can be promoted by *p*-aminophenol (Table 2, entries 21 and 22), which provides evidence for the Fe^{II}/Fe^{IV} mechanism.

Thus, a possible pathway for the formation of **5-Cbz** was proposed as shown in Scheme 4. First, under the reduction of *p*-aminophenol, Fe^{III} is reduced to Fe^{II} (the proton on the hydroxyl group of *p*-aminophenol is captured by EtMgBr), forming the intermediate **A**. **A** reacts with EtMgBr to obtain an intermediate **B** containing a C–Fe bond. **B** undergoes oxidative addition with **6** to obtain Fe^{IV}-containing intermediate **C**, which then undergoes reduction elimination to generate **5-Cbz** and obtain OTs-coordinated Fe^{II} intermediate **D**. Finally, intermediate **D** removes TsO^- to generate **A**, completing the catalytic cycle.

This possible mechanism can better explain the best reaction condition found by us. First, *p*-aminophenol is easier to donate electrons, which helps to generate Fe^{II} in the system, thus exhibiting a better yield than other ligands. Simultaneously, the use of *p*-aminophenol also requires an excessive amount of Grignard reagent to neutralize the protons dissociated from *p*-aminophenol. However, the bidentate ligands (such as 2,2'-bipy and 1,10-phenanthroline) that bind tightly to Fe are difficult to provide enough space for the exchange with EtMgBr and oxidative addition to **6** due to the catalytic center, so in terms of yield poor performance.

Conclusions

In summary, in the synthesis of upadaticinib for the treatment of rheumatoid arthritis, we optimized the scheme

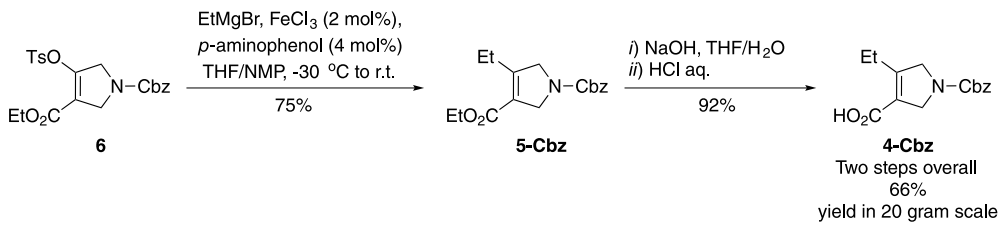

Scheme 3. Synthesis of compound **4-Cbz** from compound **6**.

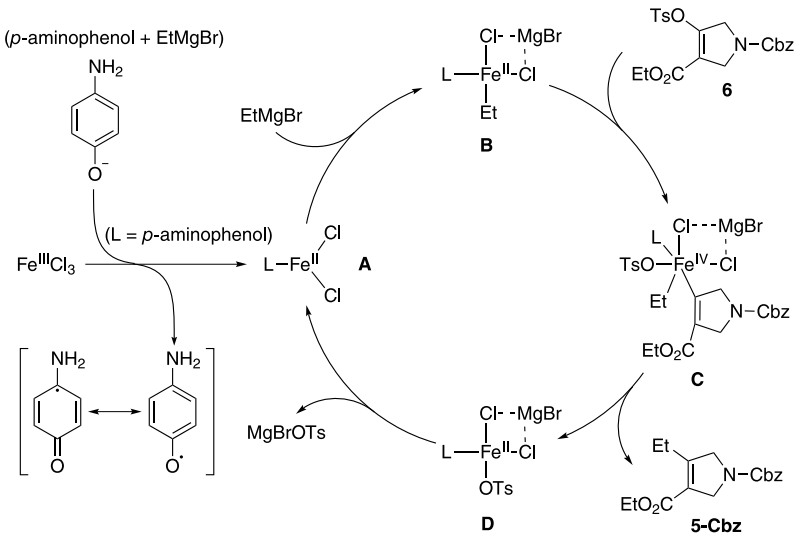

Scheme 4. Proposed reaction mechanism.

of introducing ethyl groups into the pyrroline building blocks. The use of $FeCl_3$/*p*-aminophenol catalyst system can increase the yield by 25% compared with the reported synthesis methods. In addition, we also proposed a possible mechanism for this reaction.

Experimental

All commercially available reagents were obtained from Aladdin (Shanghai, China) and all solvents were obtained from Sinopharm Chemical Reagent (Beijing, China) and used without further purification. The synthesis of compound **6** followed previous reports (Scheme S2, SI section).[14,15,17] ^{1}H nuclear magnetic resonance (NMR) spectra were recorded in dimethyl sulfoxide-d_6 (DMSO-d_6) with a Bruker 400 MHz spectrometer, tetramethylsilane (TMS) was used as an internal reference and *J* values are given in Hz. High resolution mass spectra (HRMS) were obtained on a Bruker microTOF-Q II spectrometer. PE is petroleum ether (60-90 °C).

Synthesis of 1-benzyl 3-ethyl 4-ethyl-2,5-dihydro-1*H*-pyrrole-1,3-dicarboxylate (**5-Cbz**)[17]

A mixture of 1-benzyl 3-ethyl 4-(tosyloxy)-2,5-dihydro-pyrrole-1,3-dicarboxylate (**6**, 446 mg, 1.0 mmol), anhydrous $FeCl_3$ (3.2 mg, 0.02 mmol), 4-aminophenol (4.4 mg, 0.04 mmol) and anhydrous NMP (0.1 mL) in anhydrous THF (10 mL) was cooled to −30 °C, and EtMgBr (2.0 M in THF, 0.9 mL, 1.8 mmol) was slowly added dropwise. Then, the mixture was stirred at −30 °C for 1 h and slowly raise to room temperature for 2 h. The reaction mixture was quenched with NH_4Cl sat. aq. (15 mL) and the organic phase was extracted with ethyl acetate (10 mL × 3). The organic layer was combined and washed with brine and dried over Na_2SO_4. The solvent was removed by vacuum, and the residue was purified by flash chromatography (silica gel, PE:EtOAc = 7:1) to give 227 mg (75%) of compound **5-Cbz** as a pale yellow oil. ^{1}H NMR (400 MHz, DMSO-d_6) δ 7.39-7.30 (m, 5H), 5.10 (s, 2H), 4.37-4.09 (m, 6H), 2.58 (t, *J* 7.6, 2H), 1.22 (q, *J* 7.3, 3H), 1.02 (q, *J* 7.6, 3H); HRMS (ESI-TOF) *m/z*, calcd. for $C_{17}H_{21}KNO_4$ $[M + K]^+$: 342.1108, found 342.4120.

Synthesis of 1-((benzyloxy)carbonyl)-4-ethyl-2,5-dihydro-pyrrole-3-carboxylic acid (**4-Cbz**)[17]

A mixture of **5-Cbz** (790.0 mg, 2.61 mmol) and NaOH (170 mg, 4.25 mmol) in THF and H_2O mixture solvent (6.4 mL, THF:H_2O = 1:7 v/v) was stirred at 55 °C for 2 h. After the reaction, THF was removed by vacuum and the pH was modulated to 4 by (2 M) HCl aq. The precipitate was filtered off to give 660 mg (92%) of compound **4-Cbz** as a light-yellow solid. ^{1}H NMR (400 MHz, DMSO-d_6) δ 12.63 (brs, 1H), 7.33-7.23 (m, 5H), 5.03 (s, 2H), 4.29-4.13 (m, 4H), 2.55-2.45 (m, 2H), 0.94 (q, *J* 7.6, 3H); HRMS (ESI-TOF) *m/z*, calcd. for $C_{15}H_{18}NO_4$ $[M + H]^+$: 276.1236, found 276.8720.

Supplementary Information

Supplementary information (^{1}H NMR spectra, and HRMS) are available free of charge at http://jbcs.sbq.org.br as PDF file.

Acknowledgments

This work was supported by the Fujian Provincial

Department of Science and Technology (No. 2022H0014) and the Nanping Science and Technology Bureau (No. N2020Z011).

References

1. Smolen, J. S.; Aletaha, D.; McInnes, I. B.; *Lancet* **2016**, *388*, 1984. [Crossref]
2. Combe, B.; *Best Pract. Res., Clin. Rheumatol.* **2009**, *23*, 59. [Crossref]
3. Grassi, W.; de Angelis, R.; Lamanna, G.; Cervini, C.; *Eur. J. Radiol.* **1998**, *27*, S18. [Crossref]
4. Kiu, H.; Nicholson, S. E.; *Growth Factors* **2012**, *30*, 88. [Crossref]
5. Babon, J. J.; Lucet, I. S.; Murphy, J. M.; Nicola, N. A.; Varghese, L. N.; *Biochem. J.* **2014**, *462*, 1. [Crossref]
6. Haan, C.; Ungureanu, D.; Pekkala, T.; Silvennoinen, O.; Haan, S. In *Jak-Stat Signaling: from Basics to Disease*; Decker, T.; Müller, M., eds.; Springer: Vienna, 2012. [Crossref]
7. Ivashkiv, L. B.; Hu, X. Y.; *Arthritis Res. Ther.* **2004**, *6*, 159. [Crossref]
8. O'Shea, J. J.; Holland, S. M.; Staudt, L. M.; *N. Engl. J. Med.* **2013**, *368*, 161. [Crossref]
9. Genovese, M. C.; Fleischmann, R.; Combe, B.; Hall, S.; Rubbert-Roth, A.; Zhang, Y.; Zhou, Y.; Mohamed, M.-E. F.; Meerwein, S.; Pangan, A. L.; *Lancet* **2018**, *391*, 2513. [Crossref]
10. Genovese, M. C.; Kremer, J. M.; Kartman, C. E.; Schlichting, D. E.; Xie, L.; Carmack, T.; Pantojas, C.; Burson, J. S.; Tony, H.-P.; Macias, W. L.; Rooney, T. P.; Smolen, J. S.; *Rheumatology* **2018**, *57*, 900. [Crossref]
11. Wishart, N.; Bonafoux, D. F.; Frank, K. E.; Hobson, A. D.; Konopacki, D. B.; Martinez, G. Y.; Wang, L.; *US pat. US20130072470A1*, **2013**.
12. Allian, A.; Jayanth, J.; Mohamed, M. E.; Mulhern, M.; Nordstroem, L. F.; Othman, A.; Rozema, M.; Bhagavatula, L.; Marroum, P. J.; Mayer, P. T.; *US pat. US20170129902A1*, **2017**.
13. Sampath, M.; Jayaraman, S. R.; Eda, V. R.; Potham, R.; Budhdev, R. R.; Sen, S.; Bandichhor, R.; Oruganti, S.; *Org. Process Res. Dev.* **2022**, *26*, 1794. [Crossref]
14. Allian, A.; Jayanth, J.; Mohamed, M.-E.; Mulhern, M.; Nordstroem, L. F.; Othman, A.; Rozema, M.; Bhagavatula, L.; Marroum, P. J.; Mayer, P. T.; *US pat. WO2017066775A1*, **2017**.
15. Yerva, E.; Dasari, S. R.; Shinde, D.; Gadakar, M.; Adali, L. R.; Jayachandra, S.; *IN pat. WO2020202183A1*, **2020**.
16. Zheng, X.; Zhang, Y.; Fu, C.; Wu, Y.; *CN pat. CN111217819A*, **2020**.
17. Rozema, M. J.; Bhagavatula, L.; Christesen, A.; Dunn, T. B.; Ickes, A.; Kotecki, B. J.; Marek, J. C.; Moschetta, E.; Morrill, W. H.; Mulhern, M.; Rasmussen, M.; Reynolds, T.; Yu, S.; *Org. Process Res. Dev.* **2022**, *26*, 949. [Crossref]
18. Li, P.; Wang, P.; Zhou, P.; Yao, W.; Jiang, Q.; *CN pat. CN114621127A*, **2022**.
19. Cahiez, G.; Avedissian, H.; *Synthesis* **1998**, 1199. [Crossref]
20. Bogdanović, B.; Schwickardi, M.; *Angew. Chem., Int. Ed.* **2000**, *39*, 4610. [Crossref]
21. Fürstner, A.; Leitner, A.; Méndez, M.; Krause, H.; *J. Am. Chem. Soc.* **2002**, *124*, 13856. [Crossref]
22. Agata, R.; Takaya, H.; Matsuda, H.; Nakatani, N.; Takeuchi, K.; Iwamoto, T.; Hatakeyama, T.; Nakamura, M.; *Bull. Chem. Soc. Jpn.* **2019**, *92*, 381. [Crossref]

Submitted: July 29, 2023
Published online: October 16, 2023